

## **Distribution Agreement**

In presenting this thesis as a partial fulfillment of the requirements for a degree from Emory University, I hereby grant to Emory University and its agents the non-exclusive license to archive, make accessible, and display my thesis in whole or in part in all forms of media, now or hereafter now, including display on the World Wide Web. I understand that I may select some access restrictions as part of the online submission of this thesis. I retain all ownership rights to the copyright of the thesis. I also retain the right to use in future works (such as articles or books) all or part of this thesis.

Mark Essien

April 10, 2023

Studying the Relationship Between Cellular Mechanics and Metabolism

by

Mark Essien

Khalid Salaita, PhD  
Adviser

Chemistry

Khalid Salaita, PhD  
Adviser

Antonio Brathwaite, PhD  
Committee Member

Malathy Shanmugam PhD, MS  
Committee Member

2023

Studying the Relationship Between Cellular Mechanics and Metabolism

By

Mark Essien

Khalid Salaita, PhD

Adviser

An abstract of  
a thesis submitted to the Faculty of Emory College of Arts and Sciences  
of Emory University in partial fulfillment  
of the requirements of the degree of  
Bachelor of Science with Honors

Chemistry

2023

## Abstract

### Studying the Relationship Between Cellular Mechanics and Metabolism

By Mark Essien

Mechano-transduction plays a key role in modulating cellular processes, especially in cancer cells. Past studies have illustrated that mechanical inhibition can modulate the activity of metabolic pathways, while inhibition of glycolysis and other processes can attenuate cellular mechanical activity. However, past studies fail to study the relationship between metabolism and single-molecule traction forces that occur on a pN scale. In this work, we aimed to discover the relationship between metabolism and pN traction forces by synthesizing tension gauge tether (TGT) probes, plating cells on 12 pN and 56 pN tension probes, and finally by inhibiting mechanical and metabolic activity through the use of mechanical inhibitors, blebbistatin and Y27632, and metabolic inhibitors, 2-deoxy-D-glucose (2DG) and 6-aminonicotinamide (6AN.) In summary, we discovered that TGT probes modulate ATP levels in HeLa and MEF cells, inhibition of traction forces lowers ATP levels, and blocking glycolysis and the pentose phosphate pathway leads to decreases in ATP levels. Future works could utilize DNA tension probes to study other cancer cell lines.

Studying the Relationship Between Cellular Mechanics and Metabolism

By

Mark Essien

Khalid Salaita, PhD

Adviser

A thesis submitted to the Faculty of Emory College of Arts and Sciences  
of Emory University in partial fulfillment  
of the requirements of the degree of  
Bachelor of Science with Honors

Chemistry

2023

## Acknowledgements

I would like to thank my advisor, Dr. Khalid Salaita, for allowing me to work in his lab and complete this honors thesis. Being a member of his lab allowed me to grow as a scientist. I also want to give a special thank you to each member of his lab who assisted me during the honors thesis process.

I want to give a special thank you to my mentor, Dr. Sk Aysha Rashid, for her assistance and support throughout my Salaita lab research experience.

I also want to thank my committee members, Dr. Antonio Brathwaite and Dr. Malathy Shanmugam, for taking time out of their busy schedules to serve on my honors thesis committee.

## Table of Contents

Introduction .....	1
Methods .....	9
Results and Discussion .....	12
Conclusion and Future Directions .....	26
Supplemental Data .....	27
References .....	28

## Introduction

### Mechano-transduction background

Mechano-transduction is a process where mechanical signals from a cell's outside environment, specifically the extracellular matrix (ECM), are transmitted to the interior of a cell. Signals can be transmitted bidirectionally, from the outside of a cell to the inside in "outside-in" signaling and from the inside of the cell to outside in "inside-out" signaling. External signals can be used to induce changes in cellular processes such as the cell cycle.<sup>1,2</sup> The ECM, where these signals come from, is made up of proteoglycan and other proteins such as collagen and fibronectin.<sup>3</sup>

The multi-step process of mechano-transduction begins when cells use integrins to feel their environment. Integrins are membrane protein surface receptors that contain an alpha and beta subunit (Figure #1.) A variety of subunit versions exist and thus allow cell integrins to interact with numerous components in their environment.<sup>3</sup> These integrin receptors can bind to fibronectin and other specific protein sequences.<sup>3</sup> From there, the integrin transmits the mechanical signal to the inside of the cell through the formation of focal adhesions (Figure #2.) Focal adhesions are the integrin-protein interactions that join the integrin receptors to the actin cytoskeleton components.<sup>4</sup> These interactions occur with proteins such as vinculin, talin, and paxillin<sup>4</sup> that interact with actin-myosin bundles to further transmit the mechanical signal to the side of the cell.

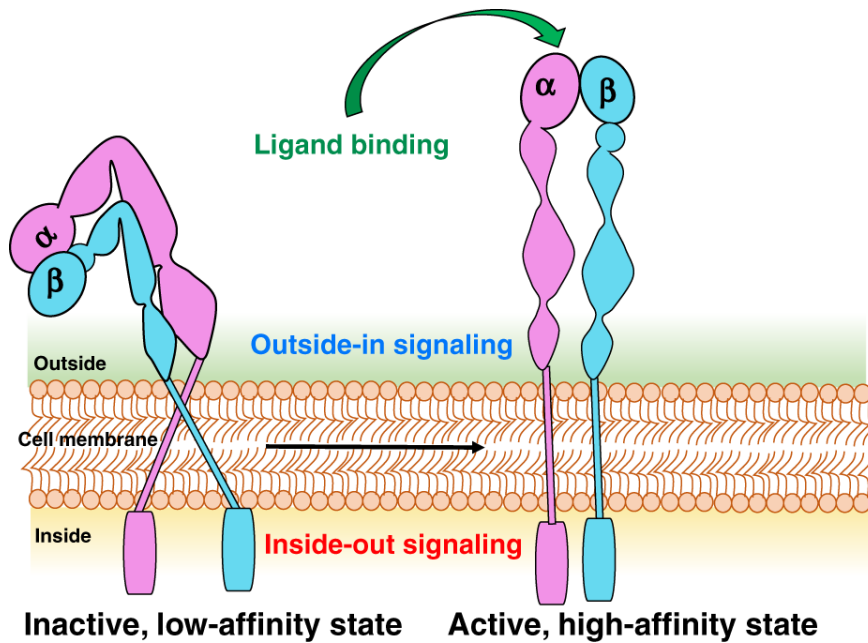


**Figure #1. Integrin structure:** The structure of integrin is depicted above. Integrin contains alpha and beta subunits that allow it to interact with a variety of environmental components. Reference: [The role of integrins in inflammation and angiogenesis](#) by [Olachi J. Mezu-Ndubuisi](#) & [Akhil Maheshwari](#) is licensed under [CC BY 4.0](#)<sup>5</sup>

After the mechanical signal has reached the inside of a cell, the cytoskeleton contractility further transmits the signal and leads to further downstream cellular effects.<sup>4,6</sup> Actin cytoskeleton slides along Myosin II proteins, leading to the formation of stress fibers.<sup>4,6</sup> Mechanical activity directly regulates myosin II activity through activation of the Rho/ROCK pathway.<sup>7,8</sup> When RhoA is in its active GTP form, Rho kinase (ROCK) is activated. The activation of ROCK leads to phosphorylation of the myosin regulatory light chain, thus promoting actin bundling. This ultimately leads to the interaction of actin and myosin.<sup>3,8,9,10,11,12</sup>

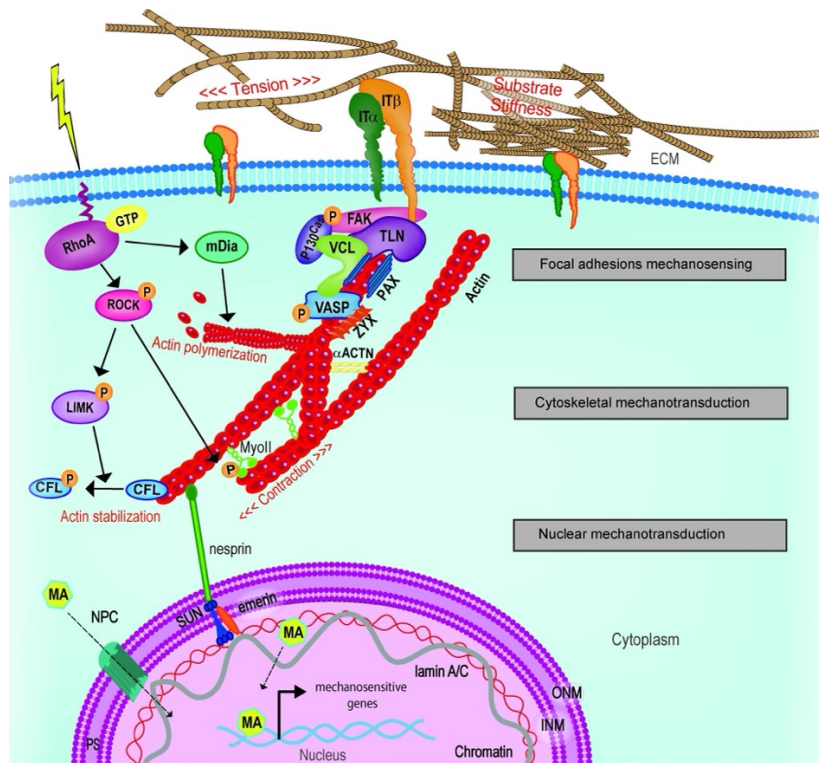


**Figure #2. Integrin-ECM interaction:** Integrin-ECM interactions are mediated by focal adhesion proteins and the activation of the ROCK pathway through Rho GTPases. Reference: [Cellular Mechanotransduction: From Tension to Function](#) by [Fabiana Martino](#) et al. is licensed under [CC BY 4.0](#)<sup>4</sup>

### Disease states and their effect on the ECM

Certain disease states can greatly change the stiffness of ECM, leading to changes in cellular activity. In lung, breast, and pancreas cells, the ECM stiffness ranges from 200-1000 Pa.<sup>13,14</sup> In cancer cells, ECM stiffness is enhanced and increases to 4-10 kPa.<sup>13,14</sup> Kraning-Rush et al. illustrated that metastatic breast cancer plated on substrates with stiffnesses ranging from 1-10 kPa had higher traction force generation compared to its non-cancerous counterpart.<sup>15</sup> Similar results were also seen in other metastatic cancer cell types tested.<sup>15</sup> Previous works have also demonstrated that the interaction between the ECM and integrins could play a key role in cancer cell metastasis and migration.<sup>16,17,18</sup>

## ECM stiffness and metabolism

Cellular metabolic activity has also been found to be regulated by ECM interactions and mechano-transduction. The metabolic activity of cancer cells is especially of interest due to its reprogramming during cancer cell development.<sup>19</sup> Specifically, the Warburg effect causes cancer cells to produce energy through fermentation even though the cell is in the presence of oxygen.<sup>3</sup> Because of this, glycolysis plays an important role in cancer cell function. In this pathway, glucose is broken down into two pyruvate molecules, leading to the production of two net ATP molecules (Figure #3.) Previous work has shown that cellular environmental stiffness can modulate the production of certain glycolytic enzymes.<sup>20</sup> Park et al. discovered that wild-type human bronchial epithelial cells (HBECs) plated on stiffer substrates had higher rates of glycolysis compared to cells plated on a softer substrate.<sup>20</sup> Furthermore, phosphofructokinase (PFK), the rate-determining enzyme in glycolysis, was found to have higher expression levels in HBECs on stiff substrates compared to those on soft substrates.<sup>20</sup> When this same study treated cells with blebbistatin, an inhibitor of myosin II, levels of PFKP-GFP, the platelet isoform of PFK, and glycolysis activity were reduced on stiff substrates.<sup>20</sup>

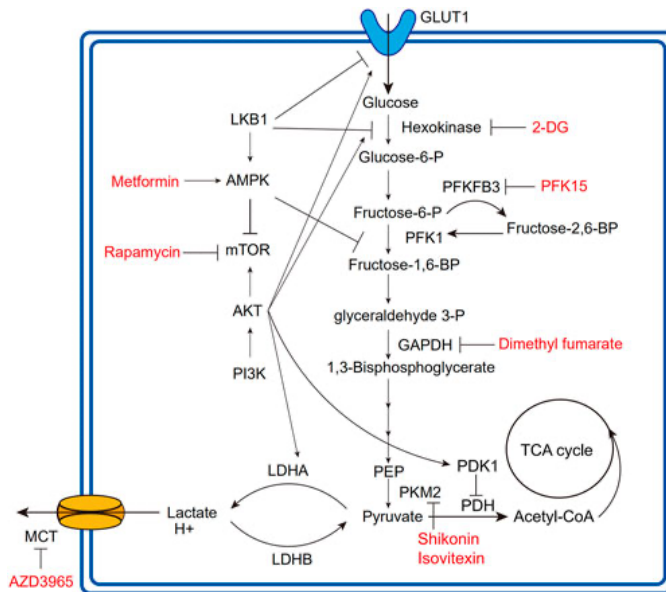


**Figure #3. Glycolysis Pathway:** Glucose is converted into glucose 6-phosphate using hexokinase (HK). This serves as a potential inhibition target. Reference: [Glycolysis in tumor microenvironment as a target to improve cancer immunotherapy](#) by [Chu Xiao](#) et al. is licensed under [CC BY 4.0](#)<sup>21</sup>

### Metabolic inhibition and its role in cellular forces

Metabolic inhibition can also play a key role in force generation. 2-deoxy-D-glucose (2DG) can act as an inhibitor of glycolysis through hexokinase (Figure #3.) Shiraishi et al. found that the use of 2DG lowered TFM force measures and mitigated focal adhesion formation in prostate cancer cells.<sup>22</sup>

In addition to its role in glycolysis, glucose also serves as a building block precursor for ribose-5-phosphate, a key building block in nucleic acids. This molecule is produced through the pentose phosphate pathway (PPP.) In the oxidative pathway of PPP, glucose-6-phosphate is converted to ribose 5-phosphate through a series of reactions (Figure #4.) The rate-determining step of this process is catalyzed by glucose 6-phosphate dehydrogenase (G6PD.)<sup>3</sup> Ribose-5-phosphate's role in nucleic acid formation makes it an important molecule in the proliferation of cancer cells. Previous studies have been conducted to illustrate the effects of PPP inhibition on

cancer cell activity. Kaushik et al. established that inhibition of G6PD through the use of 6-aminonicotinamide (6AN) led to a decrease in cellular proliferation in lung cancer cells.<sup>24</sup> Although not directly related to energy production, PPP inhibition led to lower levels of ATP in these cells as well.

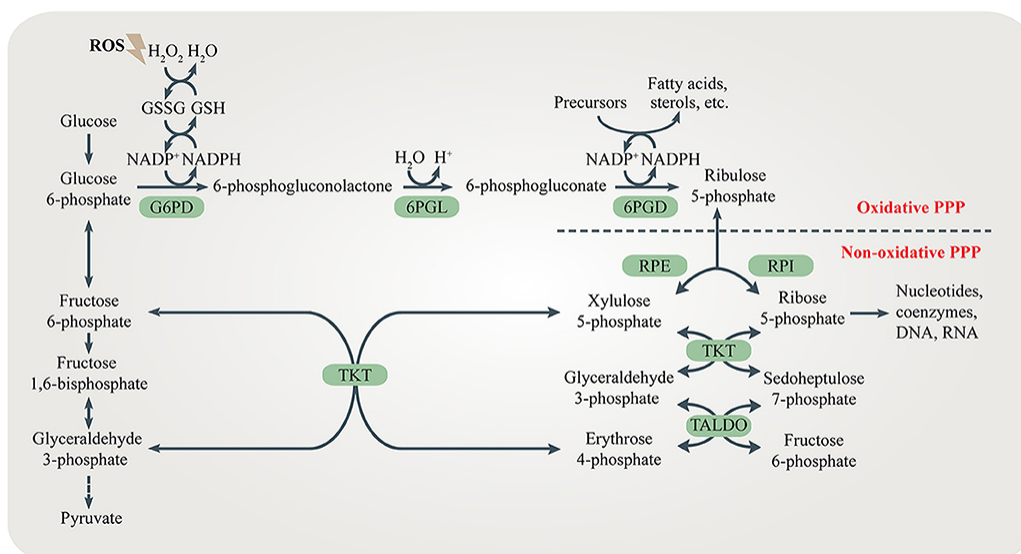


**Figure #4. The Pentose Phosphate Pathway (PPP):** The conversion of glucose 6-phosphate G6P to 6-phosphogluconolactone is catalyzed by glucose 6-phosphate dehydrogenase (G6PD) and serves as the rate-determining step of the reaction. Reference: [The Role of the Pentose Phosphate Pathway in Diabetes and Cancer](#) by Tongxin Ge et al. is licensed under [CC BY 4.0](#)<sup>25</sup>

#### DNA tension probes and current knowledge gaps

This past research has illustrated the two-way connection between metabolic activity and mechanical forces. However, despite the developments in this area, force measurements taken with TFM measure nanonewton (nN) forces, but single receptor forces occur on a piconewton (pN) scale.<sup>27,28,29,30,31,32</sup> New methods have been developed in hopes of accurately capturing these pN measurements. DNA tension probe technology, specifically tension gage tether (TGT) probes, have been developed in hopes of solving this conundrum (Figure #5.) TGT tension probes are typically created on biotin-streptavidin surfaces.<sup>27</sup> These tension probes contain two DNA strands

bound together, along with a cyclic RGD (cRGD) ligand that mimics fibronectin<sup>33</sup>, a fluorophore such as Cy3B, and a quencher such as BHQ-2.<sup>27</sup> The cRGD serves as the ligand for integrin cell surface receptors. When the DNA strand is attached, the quencher stops the fluorophore from releasing light energy. When the force threshold for the tension probe is passed, the DNA strand is unwound, and the fluorophore releases light energy. This light energy release can be quantified and serve as a measurement of traction force activity in cells. TGT probes open at different thresholds based on the structure of the probe. In 12 pN and 56 pN TGT probes, the difference in force is caused by the orientation of the biotin-binding site to the cRGD ligand. Previous work has demonstrated how DNA tension probes could be used as a drug evaluation tool<sup>34</sup> and a means to study cardiac cell maturation.<sup>35</sup>

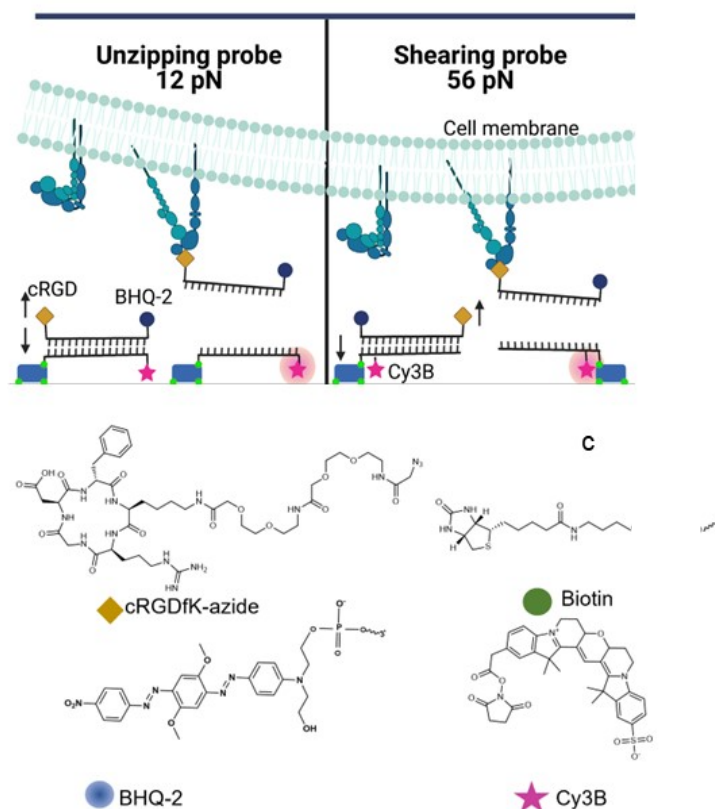


**Figure #5. Tension Gauge Tether (TGT) probes:** A. Cells can pull on TGT probes of different thresholds. When the force threshold is passed, DNA probes rupture and lead to fluorescence. B. The chemical structures contained in TGT probes. C. The probability of probes rupturing under different loading times (Adapted from Rashid et al.).<sup>35</sup>

Therefore, the goal of this paper was to utilize DNA tension probe technology to evaluate the relationship between single-molecule pN traction forces and ATP production. The first goals of our experiment were to synthesize 12 pN and 56 pN tension probes and plate cells on them to measure tension and ATP levels. Next, we worked to inhibit mechanical forces and determine the effects on ATP production. Finally, we aimed to inhibit glycolysis and the PPP, using 2DG and 6AN respectively, and determine their effects on pN tension force measurements. In this process, we hypothesized that inhibition of mechanical forces would lower ATP production and that inhibition of glycolysis and PPP would lead to a decrease in pN tension measurements.

## Methods

### Probe synthesis

TGT probes developed in previous literature work<sup>28,35,36,37,38</sup> were utilized. TGT top strands were synthesized by mixing a cRGD with top strand DNA in a reaction solution with 5 mM sodium ascorbate and 0.1  $\mu$ M preformed Cu-THPTA complex in a 25  $\mu$ L solution. After two hours, HPLC was used to purify the product.

To synthesize TGT bottom strands, Cy3B-NHS ester was added to bottom DNA strands by completing an NHS-amine coupling. Strands were then purified using HPLC.

To anneal the top and bottom strands, strands were synthesized in a 1.5:1 ratio at a 50  $\mu$ L volume in a thermocycler for approximately 25-30 minutes. After annealing, DNA strands were diluted using 1x Phosphate-Buffered Saline (PBS) and subsequently plated on surfaces.

### Surface Preparation

DNA tension probe surfaces were prepared following the procedures from previous literature sources.<sup>35</sup> Long glass slides were sonicated with ethanol for 15-20 minutes, washed with water, and then sonicated with water for another 15-20 minutes. A piranha reaction containing a 3:1 ratio of sulfuric acid and hydrogen peroxide was used to etch the slides for 20-25 minutes. Slides were subsequently washed with water 3-5 times and ethanol 3-5 times. Next, the long slides were placed in a 1% (3-Aminopropyl)triethoxysilane (APTES) (440140, Sigma-Aldrich) solution for 40-45 minutes. Afterward, the slides were washed with ethanol 3-5 times and dried using an oven. After 30 minutes, the slides were cooled and a 2 mg/ml solution of NHS-Biotin and DMSO was placed on the surfaces overnight.

After overnight biotin incubation, slides were washed with ethanol and baked for 20-25 minutes. After baking and cooling, slides were attached to a 96-well plate. Wells were washed with 1x PBS three times. A solution of 0.1 mg/ml solution of bovine serum albumin (BSA) was plated in each of the wells for 15 minutes. After incubation and another PBS washing, a 1 mg/ml solution of streptavidin/PBS was plated on each well and left for one hour. After streptavidin and PBS washing, 30  $\mu$ L of DNA was placed on each surface for 1 hour. Finally, after DNA plating, the wells were washed with 1x PBS three times and washed with cell serum containing P/S and FBS. Afterward, a density of  $\sim$ 10,000 cells was plated on each surface and left to incubate for 1-3 hours.

### **Cell Culture**

HeLa and mouse embryonic fibroblasts (MEF) were maintained in cell serum containing Dulbecco's Modified Eagle's Medium (DMEM) (10-013-CM, Corning), Penicillin-Streptomycin (P/S), and 10% fetal bovine serum (FBS.) Each cell line was grown in T25 flasks, and after reaching plate confluency, the cells were passaged.

### **Drug treatment**

HeLa and MEF cells were treated with ROCK inhibitor Y27632 (Y0503, MilliporeSigma) at a concentration of 25  $\mu$ M for 30 minutes on a shaker. These cell lines were also treated with a 15  $\mu$ M concentration of myosin II inhibitor blebbistatin (18-521, Fisher Scientific) for 30 minutes on a shaker.

In our metabolic inhibition experiments, HeLa cells were mainly utilized. HeLa cells were cultured with the cell culture highlighted above. HeLa cells were cultured with 20  $\mu$ M of 6-aminonicotinamide (6AN) (L06692-03, ThermoFisher), a PPP pathway inhibitor, or 10 mM of 2-deoxy-D-glucose (2DG) (D8375, Sigma-Aldrich) for approximately 30 minutes on a shaker. 2DG

was dissolved in water, while 6AN was dissolved in DMSO. Treated cells were then plated on 12 or 56 pN tension probes for approximately 1-3 hours.

### **Microscopy**

Cells were imaged and studied using a Nikon Eclipse Ti microscope, epi-fluorescence microscopy, and a 100x objective. Images were taken using a 561 nm laser to measure tension activity.

### **ATP assay**

ATP level measurements were taken using an ATP assay kit (ab1139, Abcam) in a microplate reader. Each plate well was incubated with 50  $\mu$ L of detergent solution. After shaking the plate at 600-700 rpm for 5 minutes, a 50  $\mu$ L substrate solution was added to each well. The plate was then shaken at 600-700 rpm for 5 minutes and then dark-adapted for another 10 minutes. Afterward, ATP levels were taken by measuring luminescence values in a microplate reader.

### **Data Analysis**

Data analysis and graph formation were performed using ImageJ, Prism, and Microsoft Excel.

## Results and Discussion

### Tension Gauge Tether (TGT) probes were purified using HPLC

Before we began our tension measurements, we needed to synthesize our TGT probes using the previously outlined protocol. The strands were then purified using HPLC. For the cRGD azide and ligand strand depicted below (Figure #6), 220 nm represents cRGD, 260 nm represents DNA, and 560 nm represents BHQ2, our quencher. For our 12 pN and 56 pN anchor strands (Figure #7), DNA is again represented by 260 nm and Cy3B, our fluorophore, is represented by 560 nm. The cRGD and ligand strand were released at ~20 minutes and ~15 minutes, respectively. Each of our anchor strands was released at approximately 12 minutes.

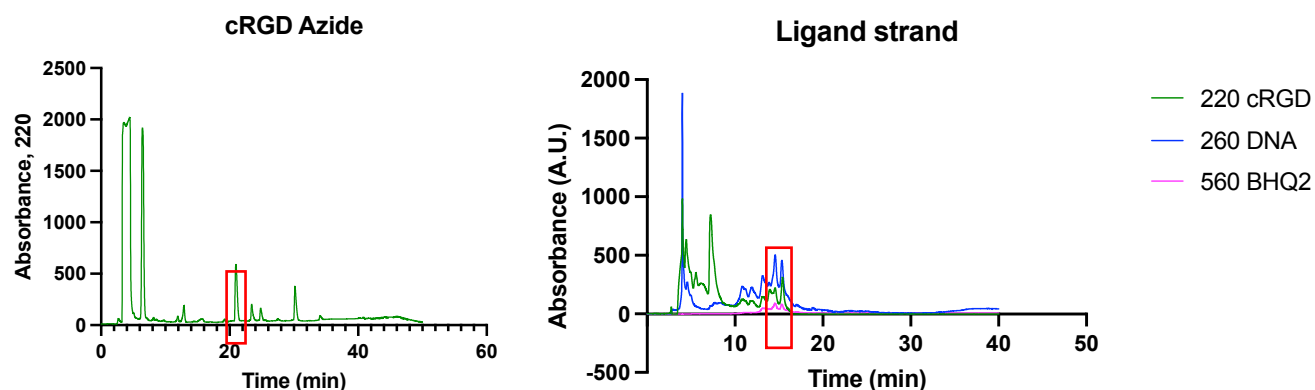


**Figure #6. cRGD azide and ligand strand purification:** The cRGD azide and ligand strands were purified using HPLC. The cRGD product was released at ~20 minutes, while the ligand strand product was released at 15 minutes.

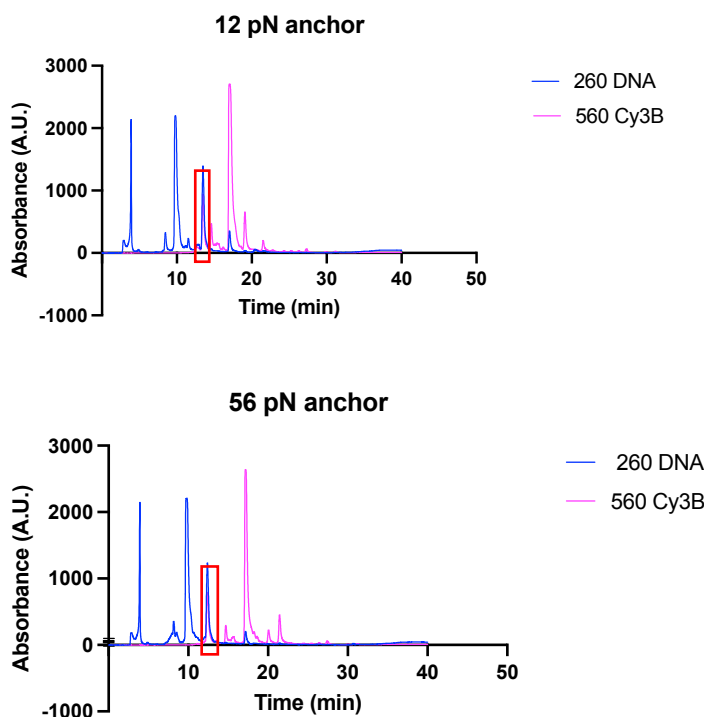


**Figure #7. Anchor strand purification:** The 12 pN and 56 pN anchor strands were purified using HPLC. Each product was released at approximately 12 minutes.

### pN tension probes modulate ATP activity

To begin our experiments, we prepared long glass slides using a piranha reaction. Afterward, we treated the surfaces with APTES and plated a biotin-DMSO solution overnight. When this treatment was completed, we attached the glass slides to a 96-well plate and added DNA tension probes to these surfaces. Then, we plated HeLa and MEF cells on these tension probe surfaces for approximately one to three hours and measured tension levels using microscopy to establish to obtain baseline values. In these measurements (Figure #8 and #9), we found that tension levels were higher for both HeLa and MEF cells plated on 12 pN probes compared to the same cells on 56 pN tension probes. This data is consistent with our initial hypothesis, where we

predicted that tension levels would be higher on 12 pN probes since these probes have a lower threshold needed to open them.

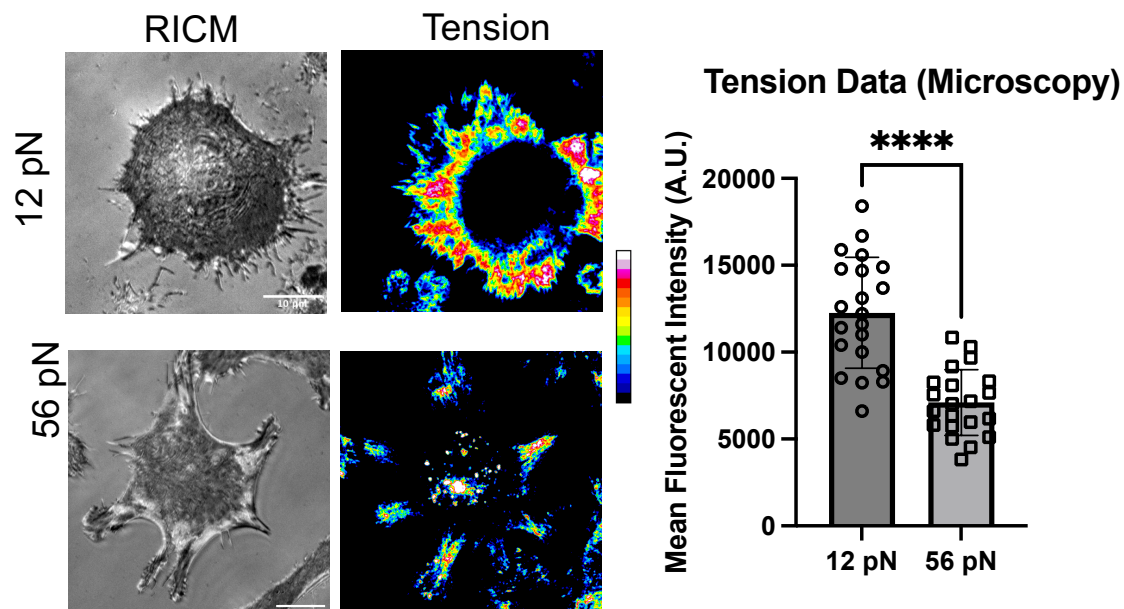


**Figure #8. Untreated MEF cell tension measurements:** Untreated MEF cell tension was taken after 1-3 hours. Tension levels were higher in cells plated on 12 pN probes.

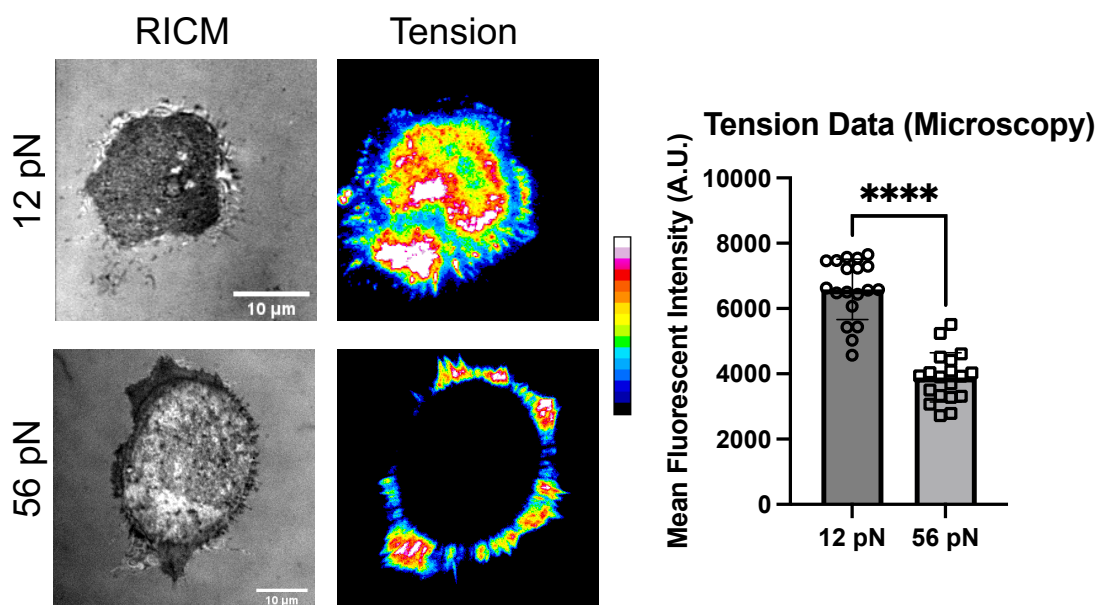


**Figure #9: Untreated HeLa tension measurements:** Untreated HeLa cell tension was taken 1-3 hours after incubation. Tension levels were elevated in cells plated on 12 pN probes.

After taking tension measurements, we measured ATP levels as means of measuring metabolic activity. To accomplish this, we utilized an ATP plate reader assay and measured the luminescence. In this assay, we found that ATP levels were higher for both HeLa and MEF cells plated on 56 pN tension probes, compared to those on 12 pN tension probes (Figure #10.) This data is also consistent with our initial predictions and hypothesis and previous literature sources, where energy production was elevated on stiffer substrates.<sup>20</sup>

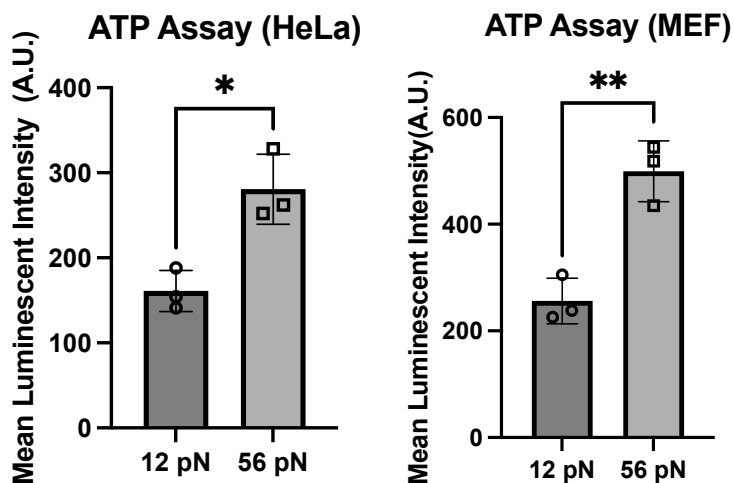


**Figure #10. ATP levels in untreated cell lines:** ATP levels were measured in HeLa and MEF cells plated on TGT probes using a microplate reader assay. In both cell lines, ATP levels were higher on 56 pN TGT probes, compared to 12 pN probes.

#### Traction force inhibition attenuates ATP activity

After taking baseline traction force measurements, we studied the effects of mechanical inhibition on ATP levels. For this experiment, we applied 15  $\mu$ M of blebbistatin to HeLa and MEF cells for approximately 30 minutes on a shaker. Blebbistatin acts as a myosin II inhibitor and stops myosin from interacting with the actin cytoskeleton. Blebbistatin inhibition treatment led to decreased cellular traction forces in both MEF and HeLa cells measured using microscopy (Figures #11 and #12.) These comparisons were taken by normalizing tension data to control values. MEF cells were also found to have a larger statistically significant difference in tension measurements in both 12 pN and 56 pN tension probes. The reduction in tension activity was consistent with our initial expectations.

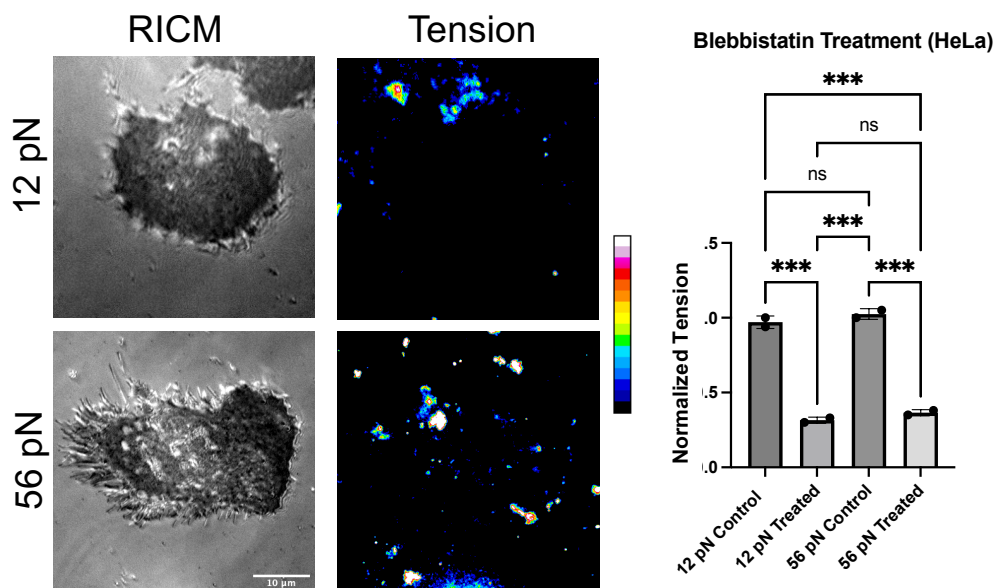


**Figure #11. Tension measurements in HeLa cells treated with Blebbistatin:** Tension measurements were taken in HeLa cells treated with blebbistatin (15  $\mu\text{M}$ ) for 30 minutes.

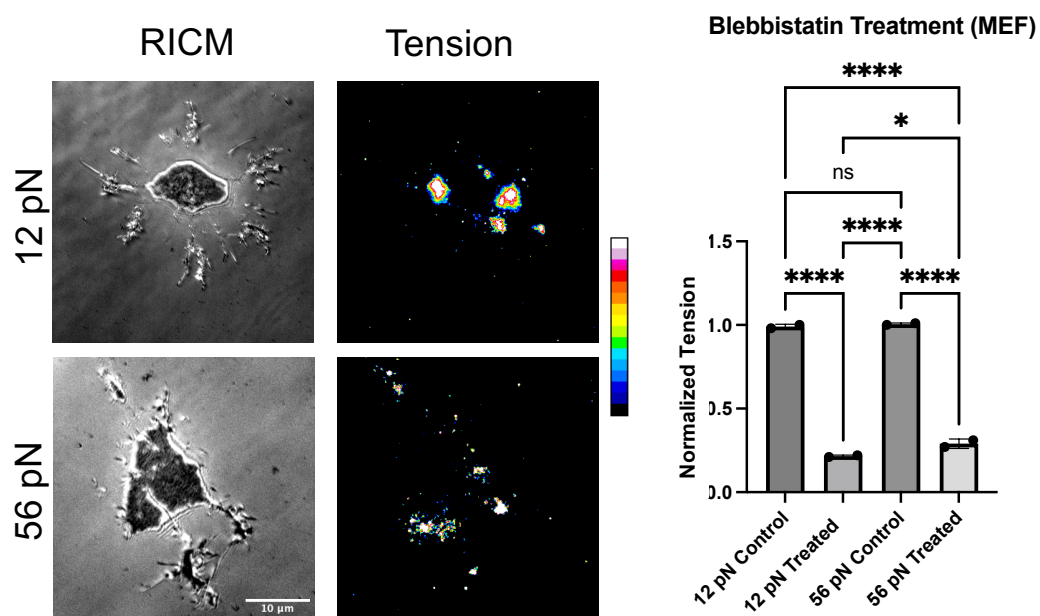


**Figure #12. Tension measurements in MEF cells treated with Blebbistatin:** Tension measurements were taken in MEF cells treated with blebbistatin (15  $\mu\text{M}$ ) for 30 minutes.

Next, we wanted to determine blebbistatin's effects on ATP production. To do this, we performed another ATP measurement assay using a microplate reader. In these cells subjected to blebbistatin inhibition, we discovered that ATP levels were reduced in both HeLa and MEF cells (Figure #13.) In both cell types, there was no difference seen in ATP levels between 12 pN and 56 pN blebbistatin-treated groups. These results illustrate that mechanical inhibition plays a role in modifying the production of ATP in both cancerous and healthy cell lines and is consistent with past studies.<sup>20</sup>

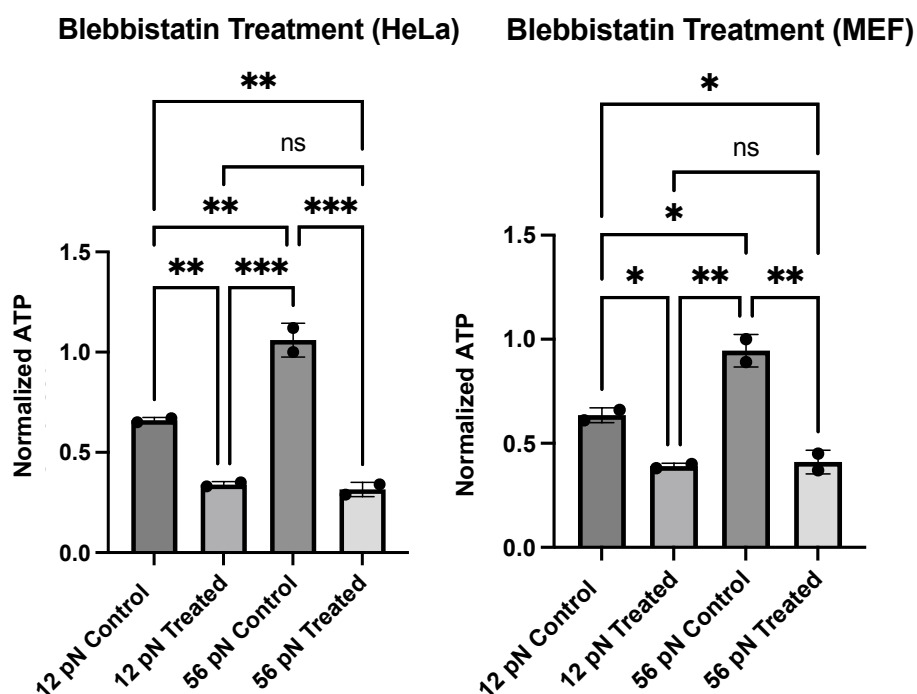


**Figure #13. ATP measurements in Blebbistatin-treated cells:** ATP measurements were taken in cell lines treated with blebbistatin (15  $\mu$ M.) ATP levels were normalized to 56 pN control values.

After our initial blebbistatin treatments, we wanted to evaluate if our results were consistent across different mechanical inhibitors utilized. In our next set of experiments, a Y27632 treatment was applied to HeLa and MEF cells to inhibit ROCK, a key kinase in the ROCK activation

pathway. This data was analyzed in the same manner described in our blebbistatin inhibition experiments. Similar to the blebbistatin treatments, tension levels were reduced in both HeLa and MEF cells treated with Y27632 (Figures #14 and #15.) MEF cells were found to have a larger statistically significant difference in treatment groups compared to HeLa cells.

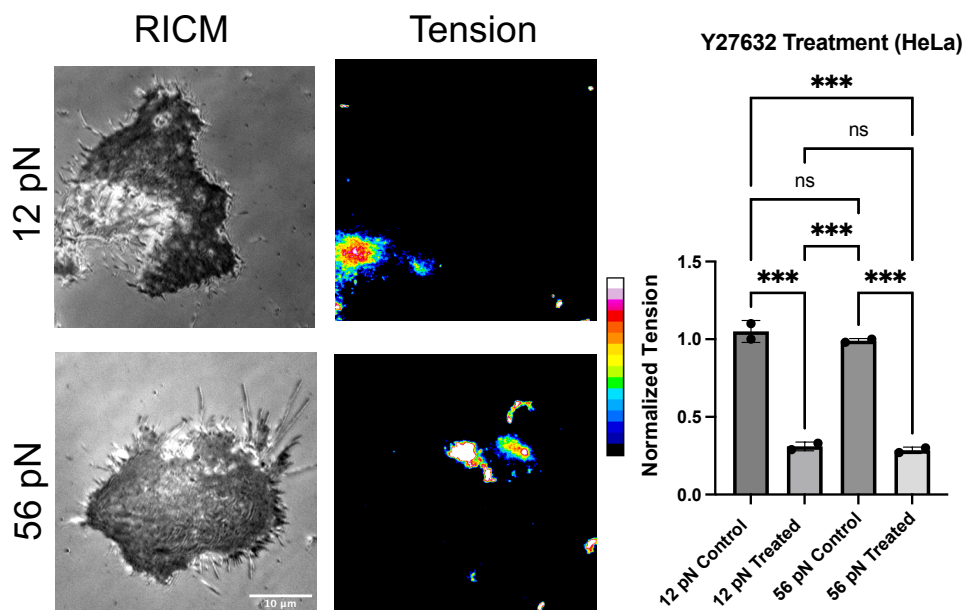


**Figure #14. Tension measurements in HeLa cells treated with Y27632:** Tension measurements were taken in HeLa treated with Y27632 (25  $\mu$ M) for 30 minutes. Tension levels were normalized to control values.

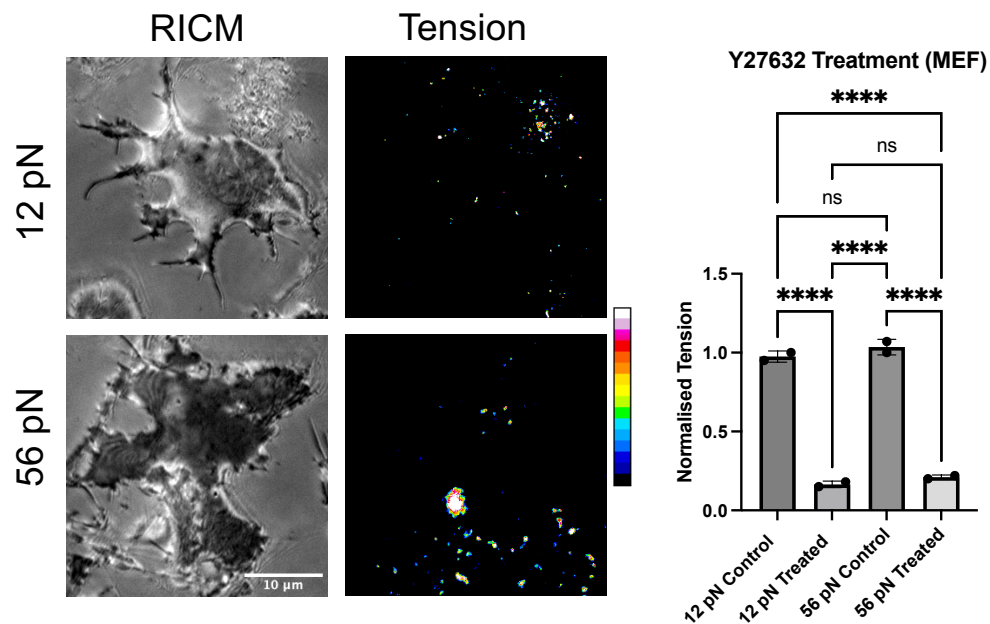


**Figure #15. Tension measurements in MEF cells treated with Y27632:** Tension measurements were taken in MEF cells treated with Y27632 (25  $\mu$ M) for 30 minutes.

After these tension measurements, we studied ATP levels using the ATP assay protocol previously discussed. In these measurements, we found that ATP levels were lower in both cell lines subjected to the Y27632 treatment (Figure #16.) Furthermore, we found that a there was larger statistically significant difference between control and treatment groups on cells plated on 56 pN treated cells compared to cells treated on 12 pN tension probes. These results further validated our metabolism-mechanics hypothesis by depicting that mechanical inhibition led to lower ATP values.

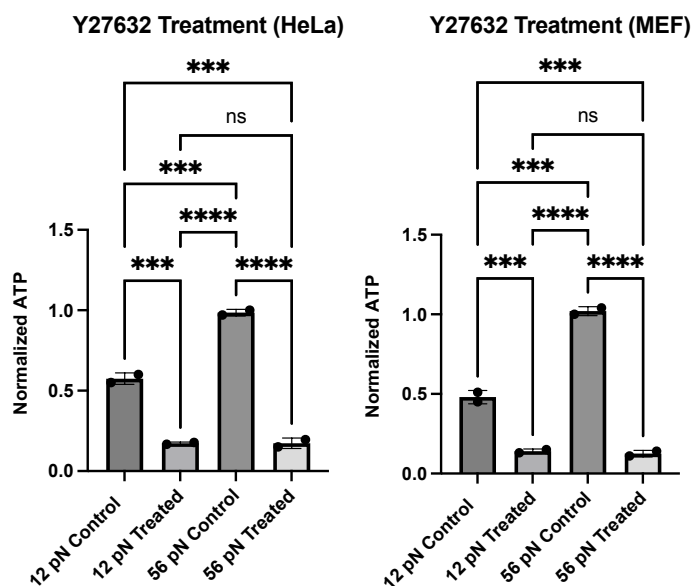


**Figure #16. ATP measurements in Y27632-treated cells:** ATP measurements were taken in cell lines treated with Y27632 (25  $\mu$ M.) ATP levels were normalized to 56 pN control values.

### Metabolic inhibition lowers cellular traction forces and ATP production

After completing our experiments with mechanical inhibition, we moved toward studying the inhibition of specific metabolic pathways. In this stage of experiments, we focused on HeLa cells since metabolic activity is known to be upregulated in cancer cells.<sup>3,19</sup> In one set of experiments, HeLa cells were treated with a 10 mM concentration of 2-deoxy-D-glucose (2DG) for 30 minutes on a shaker. In the next set of experiments, HeLa cells were treated with 20  $\mu$ M of 6-aminonicotinamide (6AN), a PPP inhibitor, following the same protocol. These inhibition concentrations were determined using previous literature studies.<sup>39,40</sup> Tension measurements were again taken using microscopy. In this data, we found that tension levels were lower in HeLa cells treated with 2DG or 6AN, compared to control groups, in cells plated on both 12 pN and 56 pN tension probes (Figures #17-20.) These results are consistent with our pre-experimental

hypothesis, where we theorized that metabolic inhibition would lower traction force activity, as seen in previous work.<sup>22</sup> In addition to our measurements of tension, we were interested in measuring the cell spread area of our HeLa cells to determine if there was any difference in treatment groups. Previous studies have indicated that tension activity can be regulated by cell spread area.<sup>41,42</sup> Similar to our tension measurements, the metabolically inhibited cells experienced decreases in cell spread area (figure #S1.)

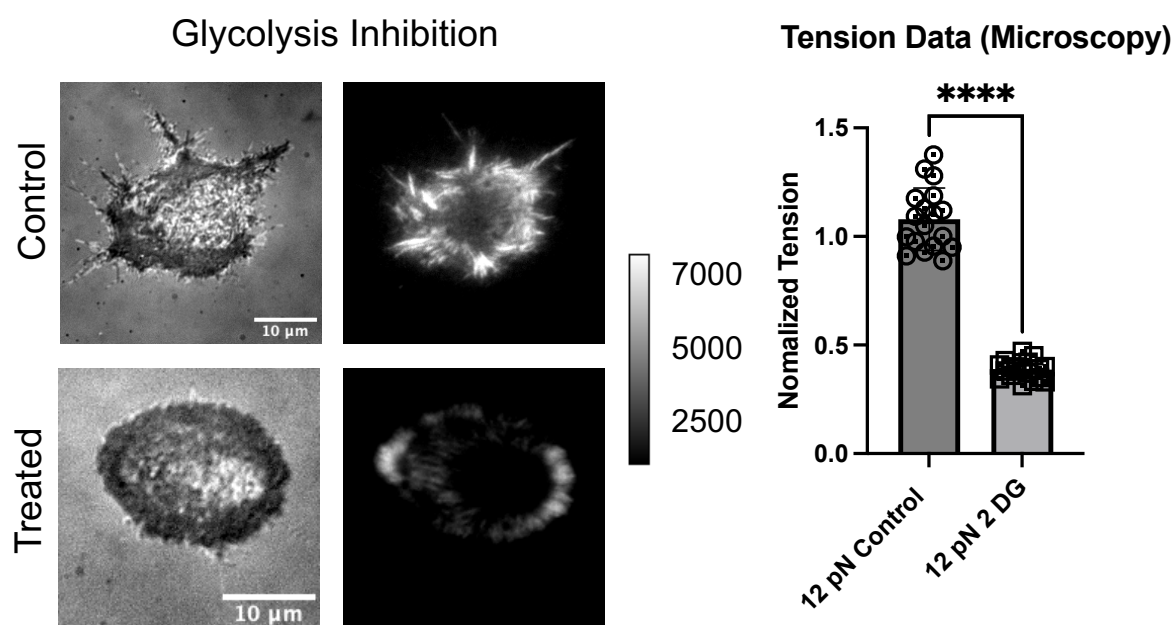


**Figure #17. Images and tension activity of HeLa cells with glycolysis inhibition on 12 pN tension probes. 10 mM of 2DG was used to inhibit glycolysis.**

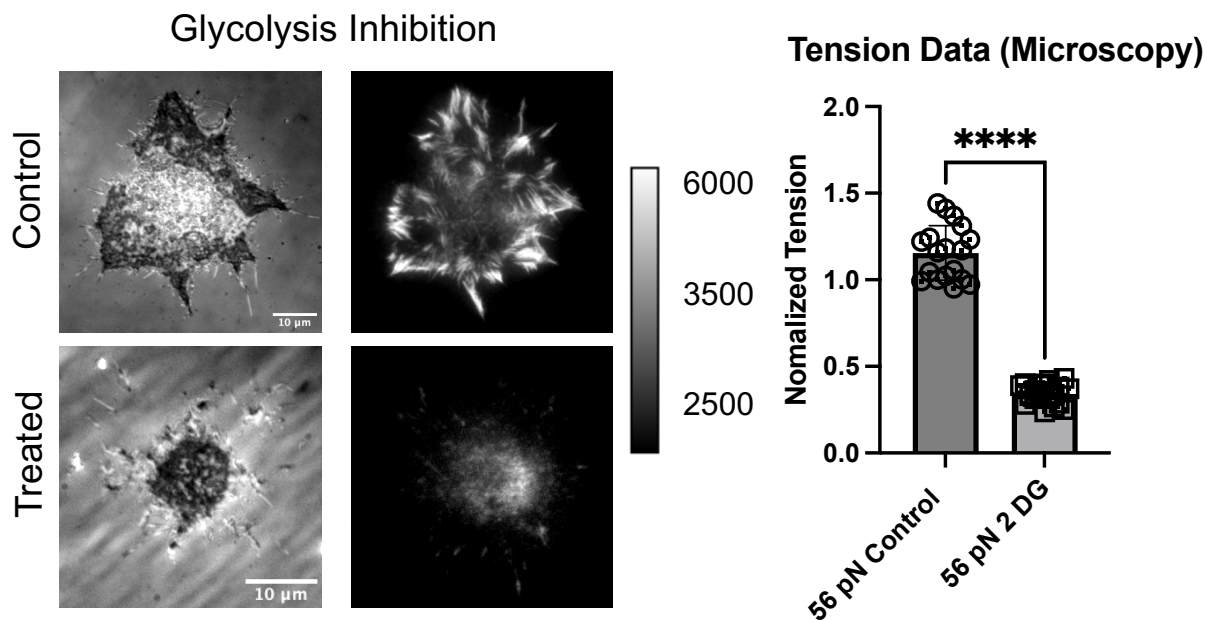


**Figure #18.** Images and tension activity of cells with glycolysis on 56 pN tension probes. 10 mM of 2DG was used to inhibit glycolysis.

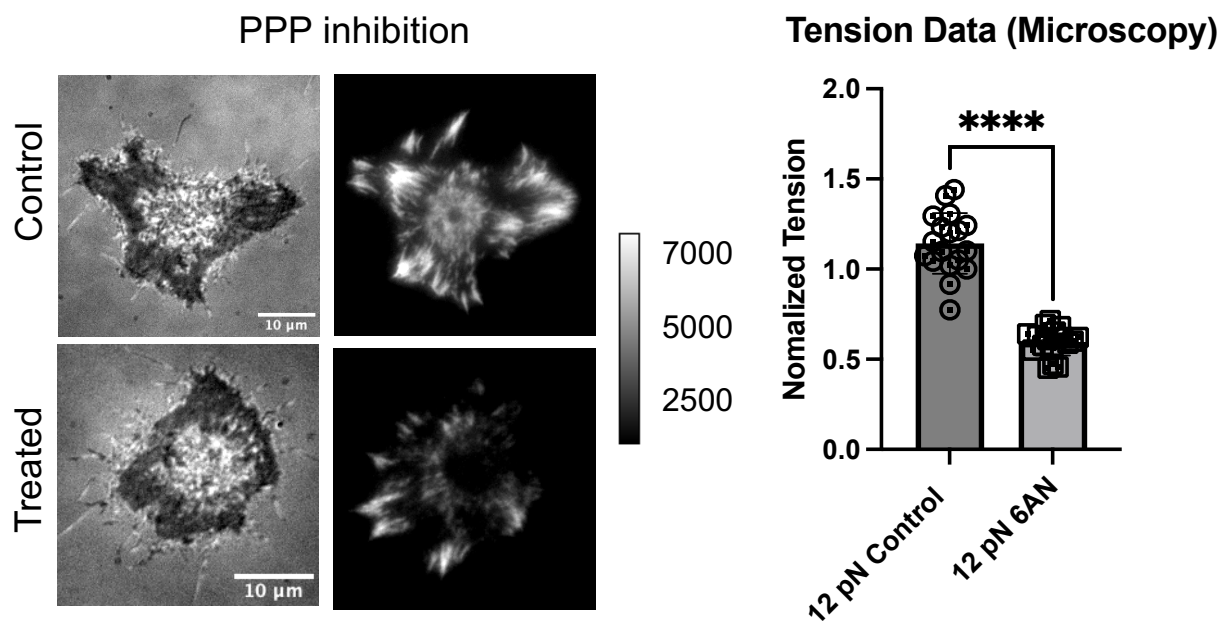


**Figure #19.** Images and tension activity of HeLa cells with PPP inhibition on 12 pN tension probes. 20  $\mu$ M of 6AN was used to inhibit PPP.

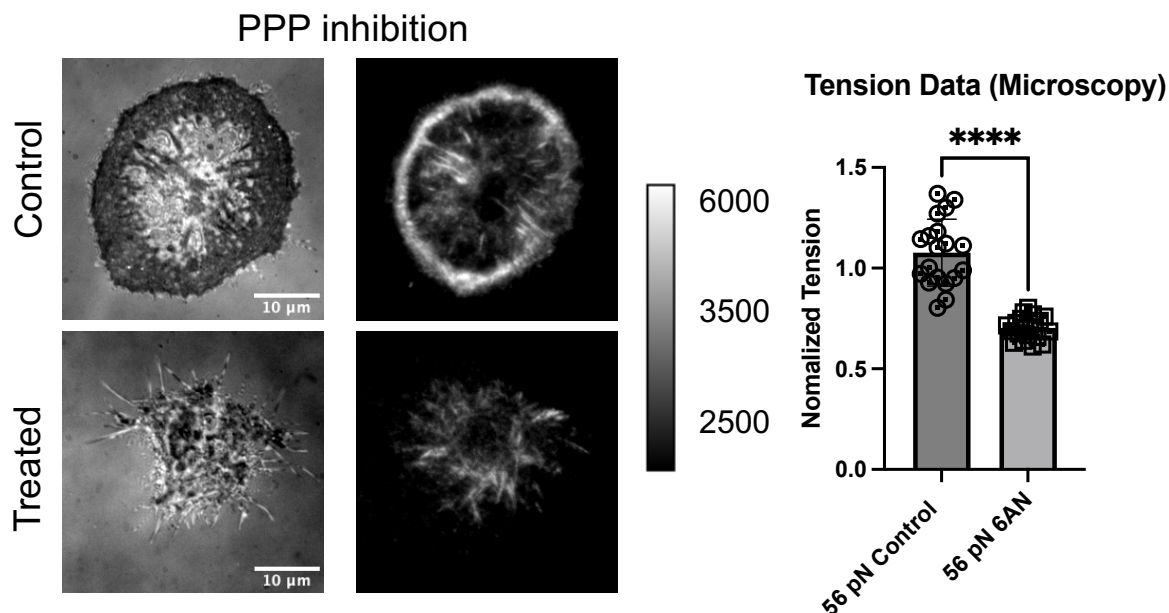


**Figure #20. Images and tension activity of cells with PPP inhibition on 56 pN tension probes. 20  $\mu$ M of 6AN was used to inhibit PPP.**

Finally, after traction force and surface area measurements, we performed an ATP assay on each treatment group. In this assay, we found that ATP levels were reduced in both 2DG and 6AN treatment groups on 12 pN and 56 pN tension probes (Figure #21.) There was not a significant difference in ATP levels between glycolysis-inhibited cells on 12 and 56 pN tension probes. Similar results were also seen with 6AN treatment groups.

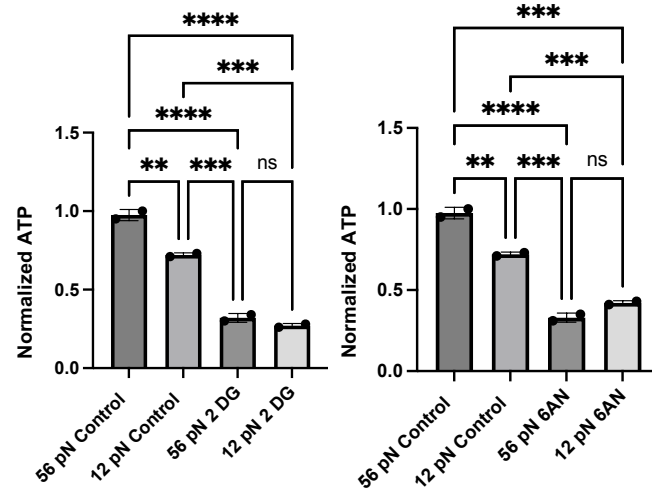


**Figure #21. ATP measurements in metabolically inhibited cells:** The ATP levels of cells treated with 2DG or 6AN. Data were normalized to 56 pN control values.

#### **Section IV – Conclusion and Future Directions**

Cancer cells have increased metabolic activity.<sup>19</sup> In addition, cancer cells with metastatic potential have higher cellular traction forces.<sup>15</sup> In this study, we have demonstrated how metabolic activity and mechano-transduction regulate each other. We have shown how plating cells in 12 pN and 56 pN tension probes can modulate ATP levels in both HeLa and MEF cell lines. Furthermore, our experiments illustrated how mechanical inhibition can result in a reduction in ATP levels. In addition, we have depicted how DNA tension probes can be utilized as a method to evaluate the effects of different metabolic treatments on single molecule receptor forces. Each metabolic inhibition led to lower traction force activity, as measured by our tension probes.

However, we mainly focused on HeLa cancer cells. Future works must study different cancer cell lines to further evaluate the usability of these tension probes. There are also multiple methods to evaluate glycolysis or metabolic inhibition through different testing kits. These tests could provide more pathway-specific data points.

## Supplemental Data

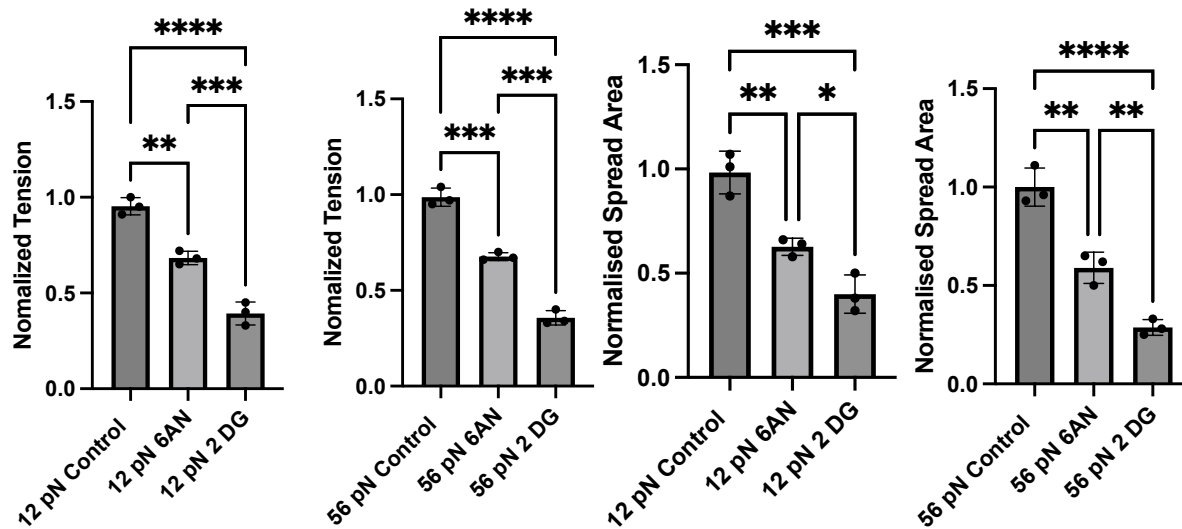


**Figure #S1. Tension summary and Cell Spread Area measurements in metabolically inhibited cells: Tension activity and cell spread area decreased in all metabolically inhibited cells.**

## References

- (1) Janmey, P. A.; Miller, R. T. Mechanisms of Mechanical Signaling in Development and Disease. *J. Cell Sci.* **2011**, *124* (1), 9–18. <https://doi.org/10.1242/jcs.071001>.
- (2) Klein, E. A.; Yin, L.; Kothapalli, D.; Castagnino, P.; Byfield, F. J.; Xu, T.; Levental, I.; Hawthorne, E.; Janmey, P. A.; Assoian, R. K. Cell-Cycle Control by Physiological Matrix Elasticity and In Vivo Tissue Stiffening. *Curr. Biol.* **2009**, *19* (18), 1511–1518. <https://doi.org/10.1016/j.cub.2009.07.069>.
- (3) Lehninger, A. L.; Nelson, D. L.; Cox, M. M. *Lehninger Principles of Biochemistry*, 6th ed.; W.H. Freeman: New York, 2013.
- (4) Martino, F.; Perestrelo, A. R.; Vinarský, V.; Pagliari, S.; Forte, G. Cellular Mechanotransduction: From Tension to Function. *Front. Physiol.* **2018**, *9*, 824. <https://doi.org/10.3389/fphys.2018.00824>.
- (5) Mezu-Ndubuisi, O. J.; Maheshwari, A. The Role of Integrins in Inflammation and Angiogenesis. *Pediatr. Res.* **2021**, *89* (7), 1619–1626. <https://doi.org/10.1038/s41390-020-01177-9>.
- (6) Romani, P.; Valcarcel-Jimenez, L.; Frezza, C.; Dupont, S. Crosstalk between Mechanotransduction and Metabolism. *Nat. Rev. Mol. Cell Biol.* **2021**, *22* (1), 22–38. <https://doi.org/10.1038/s41580-020-00306-w>.
- (7) Holle, A. W.; Engler, A. J. More than a Feeling: Discovering, Understanding, and Influencing Mechanosensing Pathways. *Curr. Opin. Biotechnol.* **2011**, *22* (5), 648–654. <https://doi.org/10.1016/j.copbio.2011.04.007>.

- (8) Burridge, K.; Monaghan-Benson, E.; Graham, D. M. Mechanotransduction: From the Cell Surface to the Nucleus via RhoA. *Philos. Trans. R. Soc. B Biol. Sci.* **2019**, *374* (1779), 20180229. <https://doi.org/10.1098/rstb.2018.0229>.
- (9) Vicente-Manzanares, M.; Choi, C. K.; Horwitz, A. R. Integrins in Cell Migration – the Actin Connection. *J. Cell Sci.* **2009**, *122* (2), 199–206. <https://doi.org/10.1242/jcs.018564>.
- (10) Amano, M.; Ito, M.; Kimura, K.; Fukata, Y.; Chihara, K.; Nakano, T.; Matsuura, Y.; Kaibuchi, K. Phosphorylation and Activation of Myosin by Rho-Associated Kinase (Rho-Kinase). *J. Biol. Chem.* **1996**, *271* (34), 20246–20249. <https://doi.org/10.1074/jbc.271.34.20246>.
- (11) Kimura, K.; Ito, M.; Amano, M.; Chihara, K.; Fukata, Y.; Nakafuku, M.; Yamamori, B.; Feng, J.; Nakano, T.; Okawa, K.; Iwamatsu, A.; Kaibuchi, K. Regulation of Myosin Phosphatase by Rho and Rho-Associated Kinase (Rho-Kinase). *Science* **1996**, *273* (5272), 245–248. <https://doi.org/10.1126/science.273.5272.245>.
- (12) Chrzanowska-Wodnicka, M.; Burridge, K. Rho-Stimulated Contractility Drives the Formation of Stress Fibers and Focal Adhesions. *J. Cell Biol.* **1996**, *133* (6), 1403–1415. <https://doi.org/10.1083/jcb.133.6.1403>.
- (13) Piersma, B.; Hayward, M.-K.; Weaver, V. M. Fibrosis and Cancer: A Strained Relationship. *Biochim. Biophys. Acta BBA - Rev. Cancer* **2020**, *1873* (2), 188356. <https://doi.org/10.1016/j.bbcan.2020.188356>.
- (14) Jiang, Y.; Zhang, H.; Wang, J.; Liu, Y.; Luo, T.; Hua, H. Targeting Extracellular Matrix Stiffness and Mechanotransducers to Improve Cancer Therapy. *J. Hematol. Oncol.* **2022**, *15* (1), 34. <https://doi.org/10.1186/s13045-022-01252-0>.

- (15) Kraning-Rush, C. M.; Califano, J. P.; Reinhart-King, C. A. Cellular Traction Stresses Increase with Increasing Metastatic Potential. *PLoS ONE* **2012**, *7* (2), e32572. <https://doi.org/10.1371/journal.pone.0032572>.
- (16) Su, C.; Li, J.; Zhang, L.; Wang, H.; Wang, F.; Tao, Y.; Wang, Y.; Guo, Q.; Li, J.; Liu, Y.; Yan, Y.; Zhang, J. The Biological Functions and Clinical Applications of Integrins in Cancers. *Front. Pharmacol.* **2020**, *11*, 579068. <https://doi.org/10.3389/fphar.2020.579068>.
- (17) Sun, Z.; Schwenzer, A.; Rupp, T.; Murdamoothoo, D.; Vegliante, R.; Lefebvre, O.; Klein, A.; Hussenet, T.; Orend, G. Tenascin-C Promotes Tumor Cell Migration and Metastasis through Integrin A9 $\beta$ 1-Mediated YAP Inhibition. *Cancer Res.* **2018**, *78* (4), 950–961. <https://doi.org/10.1158/0008-5472.CAN-17-1597>.
- (18) Casal, J. I.; Bartolomé, R. A. RGD Cadherins and A2 $\beta$ 1 Integrin in Cancer Metastasis: A Dangerous Liaison. *Biochim. Biophys. Acta BBA - Rev. Cancer* **2018**, *1869* (2), 321–332. <https://doi.org/10.1016/j.bbcan.2018.04.005>.
- (19) Zhang, D.; Li, J.; Wang, F.; Hu, J.; Wang, S.; Sun, Y. 2-Deoxy-D-Glucose Targeting of Glucose Metabolism in Cancer Cells as a Potential Therapy. *Cancer Lett.* **2014**, *355* (2), 176–183. <https://doi.org/10.1016/j.canlet.2014.09.003>.
- (20) Park, J. S.; Burckhardt, C. J.; Lazcano, R.; Solis, L. M.; Isogai, T.; Li, L.; Chen, C. S.; Gao, B.; Minna, J. D.; Bachoo, R.; DeBerardinis, R. J.; Danuser, G. Mechanical Regulation of Glycolysis via Cytoskeleton Architecture. *Nature* **2020**, *578* (7796), 621–626. <https://doi.org/10.1038/s41586-020-1998-1>.

- (21) Xiao, C.; Tian, H.; Zheng, Y.; Yang, Z.; Li, S.; Fan, T.; Xu, J.; Bai, G.; Liu, J.; Deng, Z.; Li, C.; He, J. Glycolysis in Tumor Microenvironment as a Target to Improve Cancer Immunotherapy. *Front. Cell Dev. Biol.* **2022**, *10*, 1013885. <https://doi.org/10.3389/fcell.2022.1013885>.
- (22) Shiraishi, T.; Verdone, J. E.; Huang, J.; Kahlert, U. D.; Hernandez, J. R.; Torga, G.; Zarif, J. C.; Epstein, T.; Gatenby, R.; McCartney, A.; Elisseeff, J. H.; Mooney, S. M.; An, S. S.; Pienta, K. J. Glycolysis Is the Primary Bioenergetic Pathway for Cell Motility and Cytoskeletal Remodeling in Human Prostate and Breast Cancer Cells. *Oncotarget* **2015**, *6* (1), 130–143. <https://doi.org/10.18632/oncotarget.2766>.
- (23) *2-Deoxy- D -glucose = 98 GC, crystalline 154-17-6*. <http://www.sigmaaldrich.com/> (accessed 2023-03-12).
- (24) Kaushik, N.; Kaushik, N. K.; Choi, E. H.; Kim, J. H. Blockade of Cellular Energy Metabolism through 6-Aminonicotinamide Reduces Proliferation of Non-Small Lung Cancer Cells by Inducing Endoplasmic Reticulum Stress. *Biology* **2021**, *10* (11), 1088. <https://doi.org/10.3390/biology10111088>.
- (25) Ge, T.; Yang, J.; Zhou, S.; Wang, Y.; Li, Y.; Tong, X. The Role of the Pentose Phosphate Pathway in Diabetes and Cancer. *Front. Endocrinol.* **2020**, *11*, 365. <https://doi.org/10.3389/fendo.2020.00365>.
- (26) *6-Aminonicotinamide, 99%, Thermo Scientific Chemicals*. <https://www.thermofisher.com/order/catalog/product/L06692.03> (accessed 2023-03-12).
- (27) Baek, K. Y.; Kim, S.; Koh, H. R. Molecular Tension Probes to Quantify Cell-Generated Mechanical Forces. *Mol. Cells* **2022**, *45* (1), 26–32. <https://doi.org/10.14348/molcells.2022.2049>.

- (28) Zhang, Y.; Ge, C.; Zhu, C.; Salaita, K. DNA-Based Digital Tension Probes Reveal Integrin Forces during Early Cell Adhesion. *Nat. Commun.* **2014**, *5* (1), 5167. <https://doi.org/10.1038/ncomms6167>.
- (29) Dogterom, M.; Yurke, B. Measurement of the Force-Velocity Relation for Growing Microtubules. *Science* **1997**, *278* (5339), 856–860. <https://doi.org/10.1126/science.278.5339.856>.
- (30) Fisher, M. E.; Kolomeisky, A. B. The Force Exerted by a Molecular Motor. *Proc. Natl. Acad. Sci.* **1999**, *96* (12), 6597–6602. <https://doi.org/10.1073/pnas.96.12.6597>.
- (31) Schwarz, U. S.; Balaban, N. Q.; Rivelino, D.; Bershadsky, A.; Geiger, B.; Safran, S. A. Calculation of Forces at Focal Adhesions from Elastic Substrate Data: The Effect of Localized Force and the Need for Regularization. *Biophys. J.* **2002**, *83* (3), 1380–1394.
- (32) Wiseman, P. W.; Brown, C. M.; Webb, D. J.; Hebert, B.; Johnson, N. L.; Squier, J. A.; Ellisman, M. H.; Horwitz, A. F. Spatial Mapping of Integrin Interactions and Dynamics during Cell Migration by Image Correlation Microscopy. *J. Cell Sci.* **2004**, *117* (23), 5521–5534. <https://doi.org/10.1242/jcs.01416>.
- (33) Takahashi, S.; Leiss, M.; Moser, M.; Ohashi, T.; Kitao, T.; Heckmann, D.; Pfeifer, A.; Kessler, H.; Takagi, J.; Erickson, H. P.; Fässler, R. The RGD Motif in Fibronectin Is Essential for Development but Dispensable for Fibril Assembly. *J. Cell Biol.* **2007**, *178* (1), 167–178. <https://doi.org/10.1083/jcb.200703021>.
- (34) Galior, K.; Ma, V. P.; Liu, Y.; Su, H.; Baker, N.; Panettieri, R. A.; Wongtrakool, C.; Salaita, K. Molecular Tension Probes to Investigate the Mechanopharmacology of Single Cells: A Step

- toward Personalized Mechanomedicine. *Adv. Healthc. Mater.* **2018**, *7* (14), 1800069. <https://doi.org/10.1002/adhm.201800069>.
- (35) Rashid, S. A.; Blanchard, A. T.; Combs, J. D.; Fernandez, N.; Dong, Y.; Cho, H. C.; Salaita, K. DNA Tension Probes Show That Cardiomyocyte Maturation Is Sensitive to the Piconewton Traction Forces Transmitted by Integrins. *ACS Nano* **2022**, *16* (4), 5335–5348. <https://doi.org/10.1021/acsnano.1c04303>.
- (36) Liu, Y.; Galior, K.; Ma, V. P.-Y.; Salaita, K. Molecular Tension Probes for Imaging Forces at the Cell Surface. *Acc. Chem. Res.* **2017**, *50* (12), 2915–2924. <https://doi.org/10.1021/acs.accounts.7b00305>.
- (37) Rao, T. C.; Pui-Yan Ma, V.; Blanchard, A.; Urner, T. M.; Grandhi, S.; Salaita, K.; Mattheyses, A. L. EGFR Activation Attenuates the Mechanical Threshold for Integrin Tension and Focal Adhesion Formation. *J. Cell Sci.* **2020**, jcs.238840. <https://doi.org/10.1242/jcs.238840>.
- (38) Rao, T. C.; Beggs, R. R.; Ankenbauer, K. E.; Hwang, J.; Ma, V. P.-Y.; Salaita, K.; Bellis, S. L.; Mattheyses, A. L. ST6Gal-I–Mediated Sialylation of the Epidermal Growth Factor Receptor Modulates Cell Mechanics and Enhances Invasion. *J. Biol. Chem.* **2022**, *298* (4), 101726. <https://doi.org/10.1016/j.jbc.2022.101726>.
- (39) Niccoli, S.; Boreham, D. R.; Phenix, C. P.; Lees, S. J. Non-Radioactive 2-Deoxy-2-Fluoro-D-Glucose Inhibits Glucose Uptake in Xenograft Tumours and Sensitizes HeLa Cells to Doxorubicin in Vitro. *PLOS ONE* **2017**, *12* (11), e0187584. <https://doi.org/10.1371/journal.pone.0187584>.
- (40) Hendrick, E.; Peixoto, P.; Blomme, A.; Polese, C.; Matheus, N.; Cimino, J.; Frère, A.; Mouithys-Mickalad, A.; Serteyn, D.; Bettendorff, L.; Elmoualij, B.; De Tullio, P.; Eppe, G.;

Dequiedt, F.; Castronovo, V.; Mottet, D. Metabolic Inhibitors Accentuate the Anti-Tumoral Effect of HDAC5 Inhibition. *Oncogene* **2017**, *36* (34), 4859–4874. <https://doi.org/10.1038/onc.2017.103>.

(41) Messi, Z.; Bornert, A.; Raynaud, F.; Verkhovsky, A. B. Traction Forces Control Cell-Edge Dynamics and Mediate Distance Sensitivity during Cell Polarization. *Curr. Biol.* **2020**, *30* (9), 1762-1769.e5. <https://doi.org/10.1016/j.cub.2020.02.078>.

(42) Oakes, P. W.; Banerjee, S.; Marchetti, M. C.; Gardel, M. L. Geometry Regulates Traction Stresses in Adherent Cells. *Biophys. J.* **2014**, *107* (4), 825–833. <https://doi.org/10.1016/j.bpj.2014.06.045>.

Figure #5 reference: Adapted with permission from Rashid, S. A.; Blanchard, A. T.; Combs, J. D.; Fernandez, N.; Dong, Y.; Cho, H. C.; Salaita, K. DNA Tension Probes Show That Cardiomyocyte Maturation Is Sensitive to the Piconewton Traction Forces Transmitted by Integrins. *ACS Nano* **2022**, *16* (4), 5335–5348. <https://doi.org/10.1021/acsnano.1c04303>. Copyright 2023 American Chemical Society.

